Supplementary Methods

MRI Acquisitions

The main scanning parameters are summarized below. Parameters for the dMRI scan were as follows: TR = 5520 ms, TE = 89.5 ms, FA = 78 °, 1.25 × 1.25 × 1.25 mm voxels, FOV = 210 ×180 mm, and the full dMRI session included 6 runs, representing 3 different gradient tables, with each table acquired once with right-to-left and left-to-right phase encoding polarities. Each gradient table included approximately 90 diffusion weighted directions plus 6 b = 0 acquisitions interspersed throughout each run. Diffusion weighting consisted of 3 shells of b = 1000, 2000, and 3000 s/mm^2 interspersed with an approximately equal number of acquisitions on each shell within each run. Resting-state fMRI consisted of gradient-echo echo planar imaging (EPI) sensitive to blood oxygenation level dependent (BOLD) contrast. Parameters for the rfMRI data were: TR = 720 ms, TE = 33.1 ms, FA = 52 °, 2 × 2 × 2 mm voxels, FOV = 208 × 180 mm, and 72 oblique axial slices that alternated between phase encoding in a right to left direction in one run and phase encoding in a left to right direction in the other run. Each functional run lasted 14.55 min (1200 time points). The structural T1-weighted images were collected with a 3D magnetization-prepared rapid acquisition with gradient echo (MPRAGE) sequence (sagittal plane; TR = 2400 ms; TE = 2.14 ms; TI = 1000 ms; iPAT = 2; 0.7 mm isotropic voxels, 256 interleaved slices; FOV = 224 mm; flip angle = 8 °; time = 7:40 min). T2-weighted images were collected with a T2 sampling perfection with application optimized contrasts (SPACE) sequence using different flip angle evolutions (TR = 3200; TE = 565 ms; iPAT = 2; 0.7 mm isotropic voxels, 256 interleaved slices; FOV = 224 mm; variable flip angle; time = 8:24 min)..

Data Preprocessing

The HCP MRI data preprocessing pipelines are primarily built using tools from the FMRIB Software Library (FSL) and FreeSurfer software (http://surfer.nmr. mgh.harvard.edu). We have summarized the

main steps of the data preprocessing pipeline below.

Structural MRI: The structural images first went through the HCP *PreFreeSurfer* pipeline which performed gradient distortion correction, alignment, averaging of the two sets of T1- and T2-weighted scans, brain extraction, readout distortion correction, and bias field correction, followed by registration to Montreal Neurological Institute (MNI) space. Next, the grey matter was parcellated into 34 cortical regions of interest (ROIs) per hemisphere and 14 subcortical ROIs based on the Desikan-Killiany (DK) atlas. Finally, the processed cortical and subcortical volumetric results in individual space were wrapped into standard MNI space.

Diffusion MRI: The HCP diffusion images were processed by the HCP *Diffusion Preprocessing* pipeline using the FMRIB diffusion toolbox (FSL 5.0; http://www.fmrib.ox.ac.uk/fsl). Images were corrected for motion and eddy current distortions. After intensity normalization, the b0 images of both phase-encoding directions (i.e., left-to-right and right-to-left) were used to calculate EPI susceptibility-induced field distortions, which were modeled using the eddy tool of FSL, and then corrected.

Resting-state fMRI: During the resting-state scan, the subjects underwent two runs of passive fixation (FIX) in each of two separate sessions. In each session, the phase encoding was in a right to left direction in one run and in a left to right direction in the other run. In this study, we chose the data from session 1 with the left to right phase encoding. These time series data were preprocessed using tools from FSL and FreeSurfer to implement gradient unwarping, motion correction, fieldmap-based EPI distortion correction, brain-boundary-based registration of EPI to a structural T1-weighted scan, non-linear registration into MNI space, and grand-mean intensity normalization. Following FIX-denoising, we then further processed rfMRI data using FSL and the Analysis of Functional NeuroImages (AFNI) by (1) band-pass filtering of the time-series ($0.01\ \text{Hz} < f < 0.1\ \text{Hz}$); (2) regressing the nuisance signals including the (rigid) head rigid motion parameters, white matter mean signal, cerebrospinal fluid mean signal, and global mean signal; and (3) spatial smoothing the residuals using a 4 mm full-width at half-maximum (FWHM) Gaussian kernel.

Supplementary Table

Initial Seed Masks		FreeSurfer Desikan-Killiany Atlas
1	SFG, Superior Frontal Gyrus	Superior Frontal Gyrus
2	MFG, Middle Frontal Gyrus	Anterior and Posterior part of Middle Frontal Gyrus
3	IFG, Inferior Frontal Gyrus	Pars Opercularis, Pars Triangularis
4	OrG, Orbital Gyrus	Pars Orbitalis, Lateral and Medial Divisions of Orbital Gyrus, Frontal Pole
5	PrG, Precentral Gyrus	Precentral Gyrus
6	PCL, Paracentral Lobule	Paracentral Lobule
7	STG, Superior Temporal Gyrus	Superior Temporal Gyrus, Temporal Pole, Transverse Temporal Cortex
8	MTG, Middle Temporal Gyrus	Middle Temporal Gyrus
9	ITG, Inferior Temporal Gyrus	Inferior Temporal Gyrus
10	FuG, Fusiform Gyrus	Fusiform Gyrus
11	PhG, Parahippocampal Gyrus	Entorhinal Area, Parahippocampal Gyrus
12	Psts, Posterior Superior Temporal Sulcus	Banks of the Superior Temporal Sulcus
13	SPL, Superior Parietal Lobule	Superior Parietal Lobule
14	IPL, Inferior Parietal Lobule	Inferior Parietal Lobule, Supramarginal Gyrus
15	Pcun, Precuneus	Precuneus Cortex
16	PoG, Postcentral Gyrus	Postcentral Gyrus
17	INS, Insular Gyrus	Insular Cortex
18	CG, Cingulate Gyrus	Anterior Cingulate Gyrus, Posterior Cingulate Gyrus, Caudal Part of Anterior Cingulate Gyrus, Isthmus of Cingulate Gyrus
19	MVOcC, MedioVentral Occipital Cortex	Cuneus Cortex, Pericalcarine Cortex, Lingual Gyrus
20	LOcC, Lateral Occipital Cortex	Lateral Occipital Gyrus
21	Amyg, Amygdala	Amygdala
22	Hipp, Hippocampus	Hippocampus
23	BG, Basal Ganglia	Caudate Nucleus, Putamen, Globus Pallidus, Nucleus Accumbens
24	Tha, Thalamus	Thalamus

Table S1. Modified Desikan–Killiany Labeling Protocol for the Definition of Seed Masks

After the initial parcellation using FreeSurfer, we created a variant of the DK protocol with 20 cortical regions and 4 subcortical structures per hemisphere.

Supplementary Figures and Legends

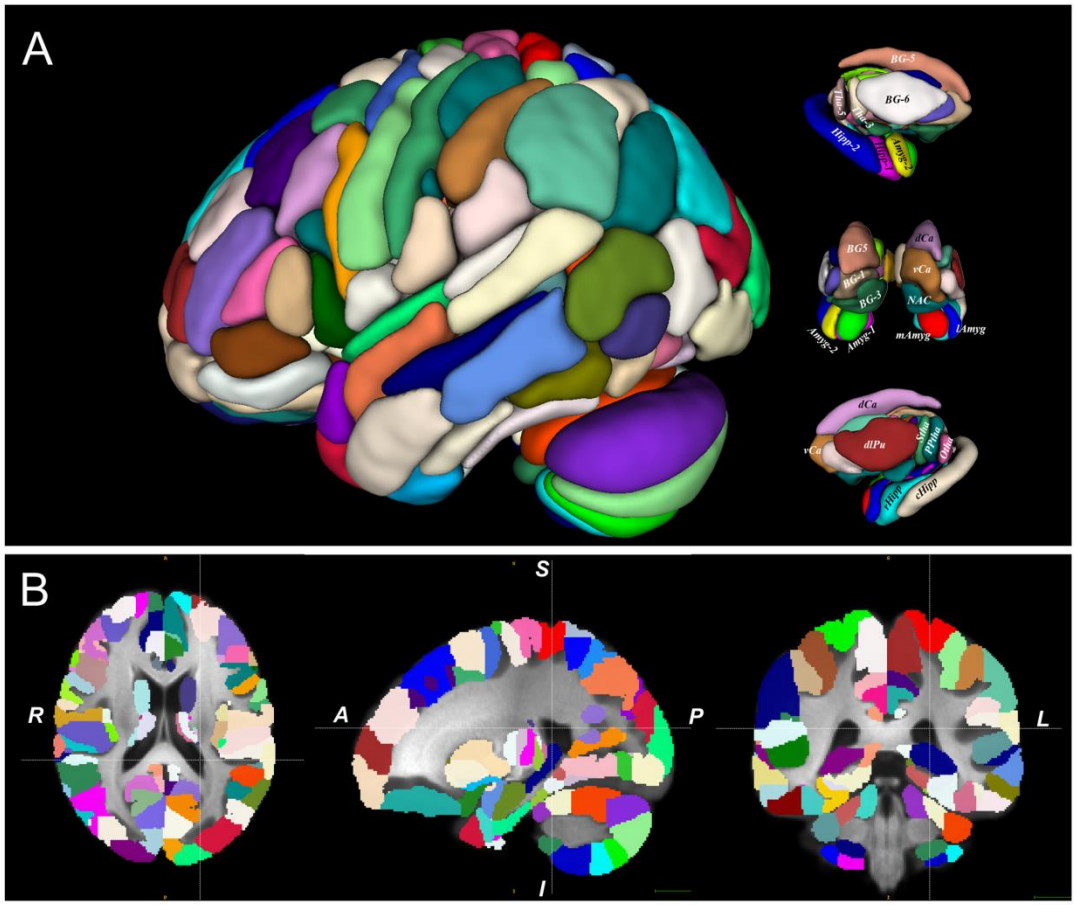

Figure S1. Brainnetome Atlas Combined with Probabilistic Cerebellar Atlas

The maximum probability map is visualized using 3D rendering (A) and slice view (B) using ITK-SNAP. A probabilistic cerebellar atlas with 28 anatomical structural subregions (http://www.icn.ucl.ac.uk/motorcontrol/imaging/suit.htm) was combined with the Brainnetome Atlas.

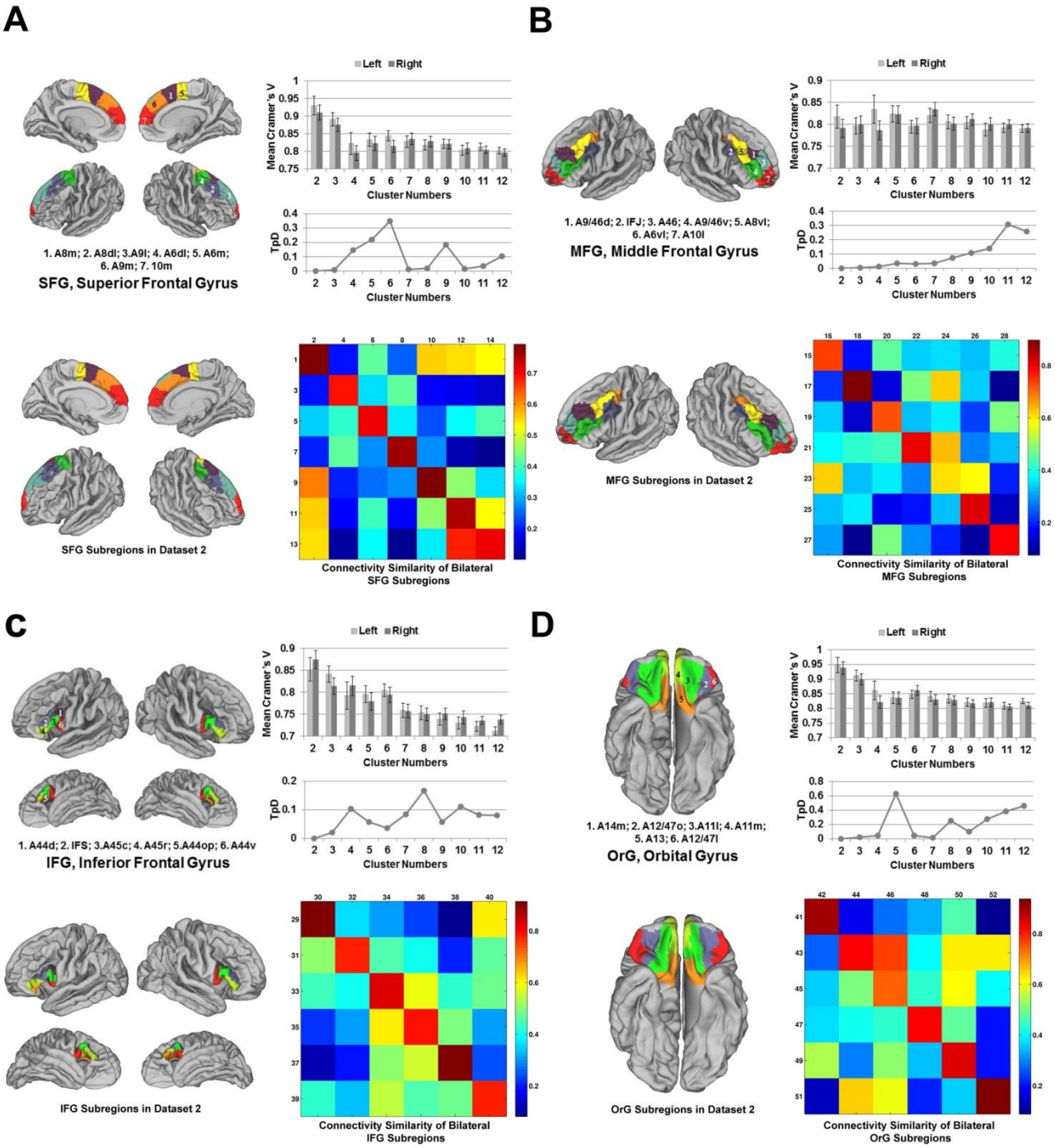

Figures S2. The Maximum Probability Maps of the Human Brainnetome Atlas Subregions in two Independent Datasets along with the Cramer's V, the Topological Distance (TpD), and the Connectivity Similarity Matrix of Bilateral Subregions: A. SFG, Superior Frontal Gyrus; B. MFG, Middle Frontal Gyrus; C. IFG, Inferior Frontal Gyrus; D. OrG, Orbital Gyrus.

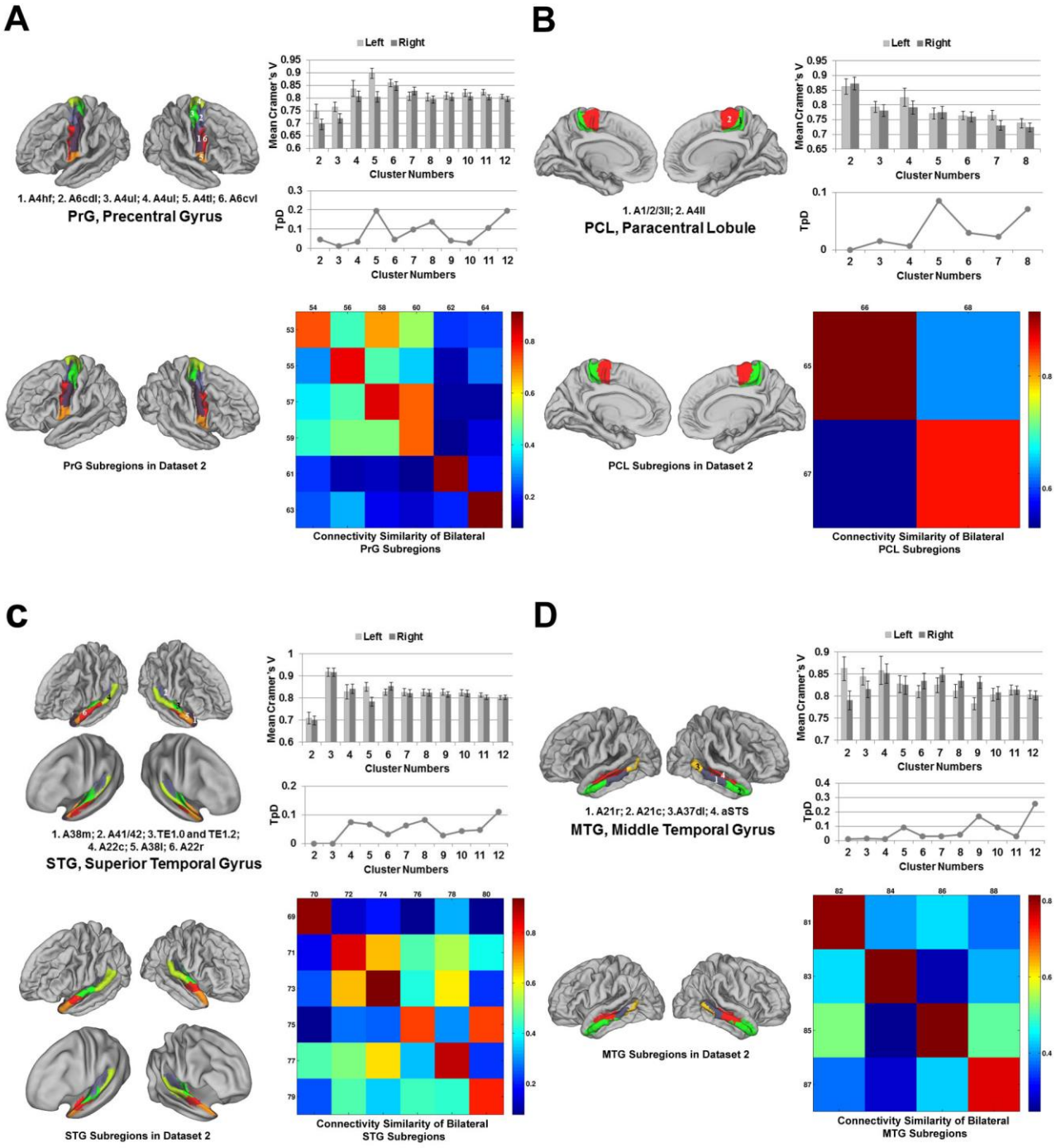

Figures S3. The Maximum Probability Maps of the Human Brainnetome Atlas Subregions in two Independent Datasets along with the Cramer's V, the Topological Distance (TpD), and the Connectivity Similarity Matrix of Bilateral Subregions: A. PrG, Precentral Gyrus; B. PCL, Paracentral Lobule; C. STG, Superior Temporal Gyrus; D. MTG, Middle Temporal Gyrus.

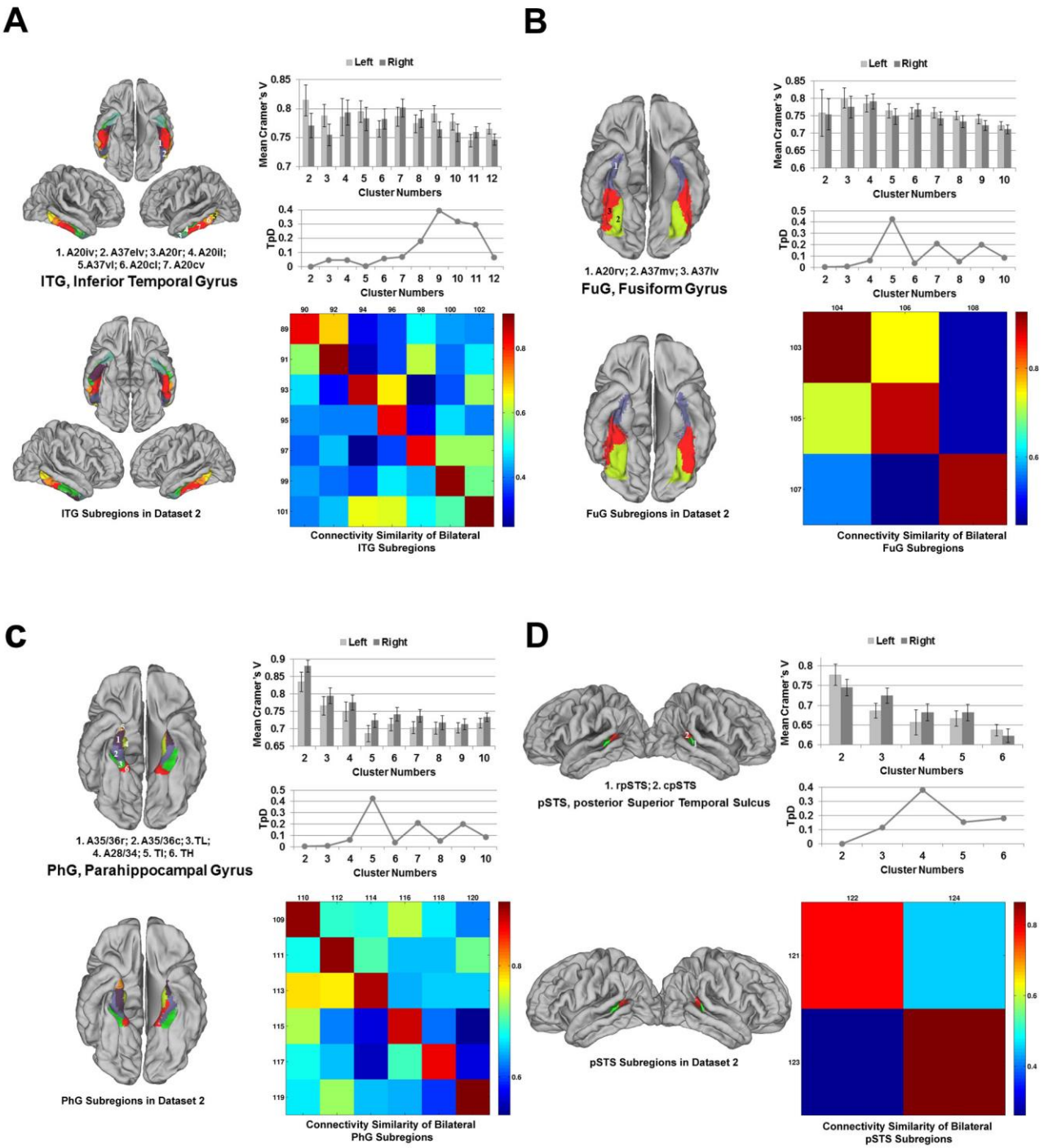

Figures S4. The Maximum Probability Maps of the Human Brainnetome Atlas Subregions in two Independent Datasets along with the Cramer's V, the Topological Distance (TpD), and the Connectivity Similarity Matrix of Bilateral Subregions: A. ITG, Inferior Temporal Gyrus; B. FuG, Fusiform Gyrus; C. PhG, Parahippocampal Gyrus; D. pSTS, posterior Superior Temporal Sulcus.

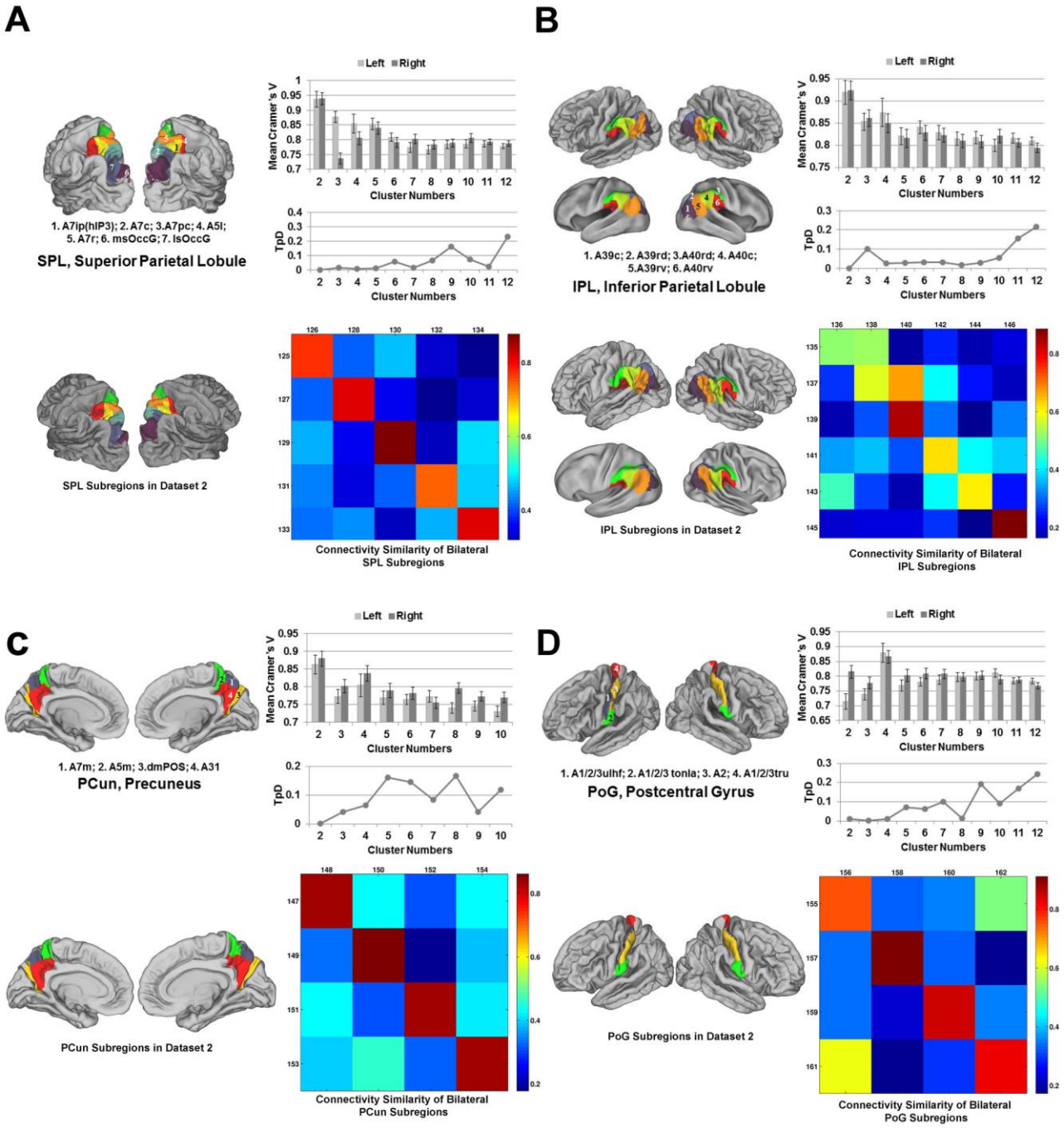

Figures S5. The Maximum Probability Maps of the Human Brainnetome Atlas Subregions in two Independent Datasets along with the Cramer's V, the Topological Distance (TpD), and the Connectivity Similarity Matrix of Bilateral Subregions: A. SPL, Superior Parietal Lobule; B. IPL, Inferior Parietal Lobule; C. PCun, Precuneus; D. PoG, Postcentral Gyrus;

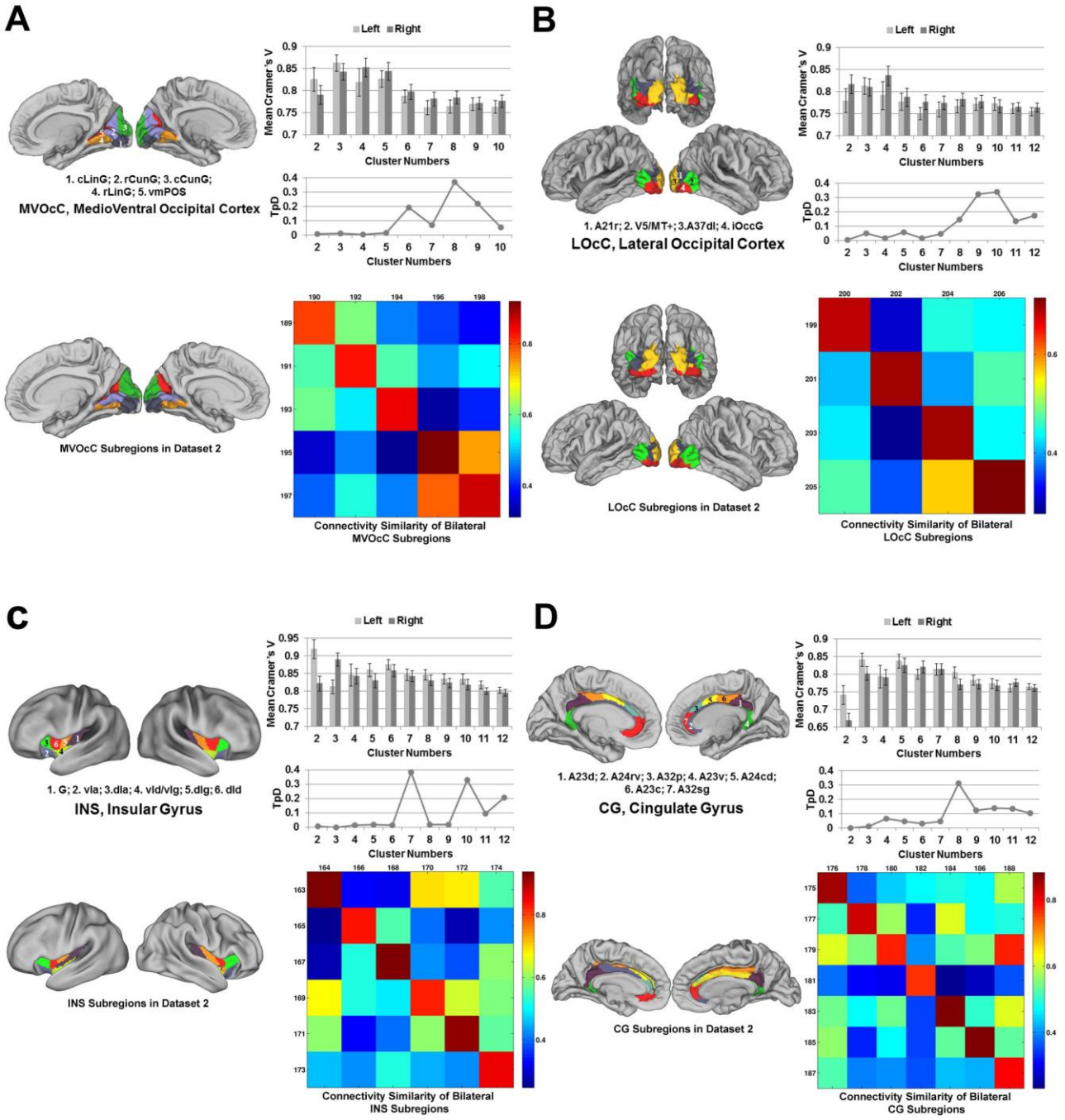

Figures S6. The Maximum Probability Maps of the Human Brainnetome Atlas Subregions in two Independent Datasets along with the Cramer's V, the Topological Distance (TpD), and the Connectivity Similarity Matrix of Bilateral Subregions: A. MVOcC, MedioVentral Occipital Cortex; B. LOcC, Lateral Occipital Cortex; C. INS, Insular Gyrus; D. CG, Cingulate Gyrus.

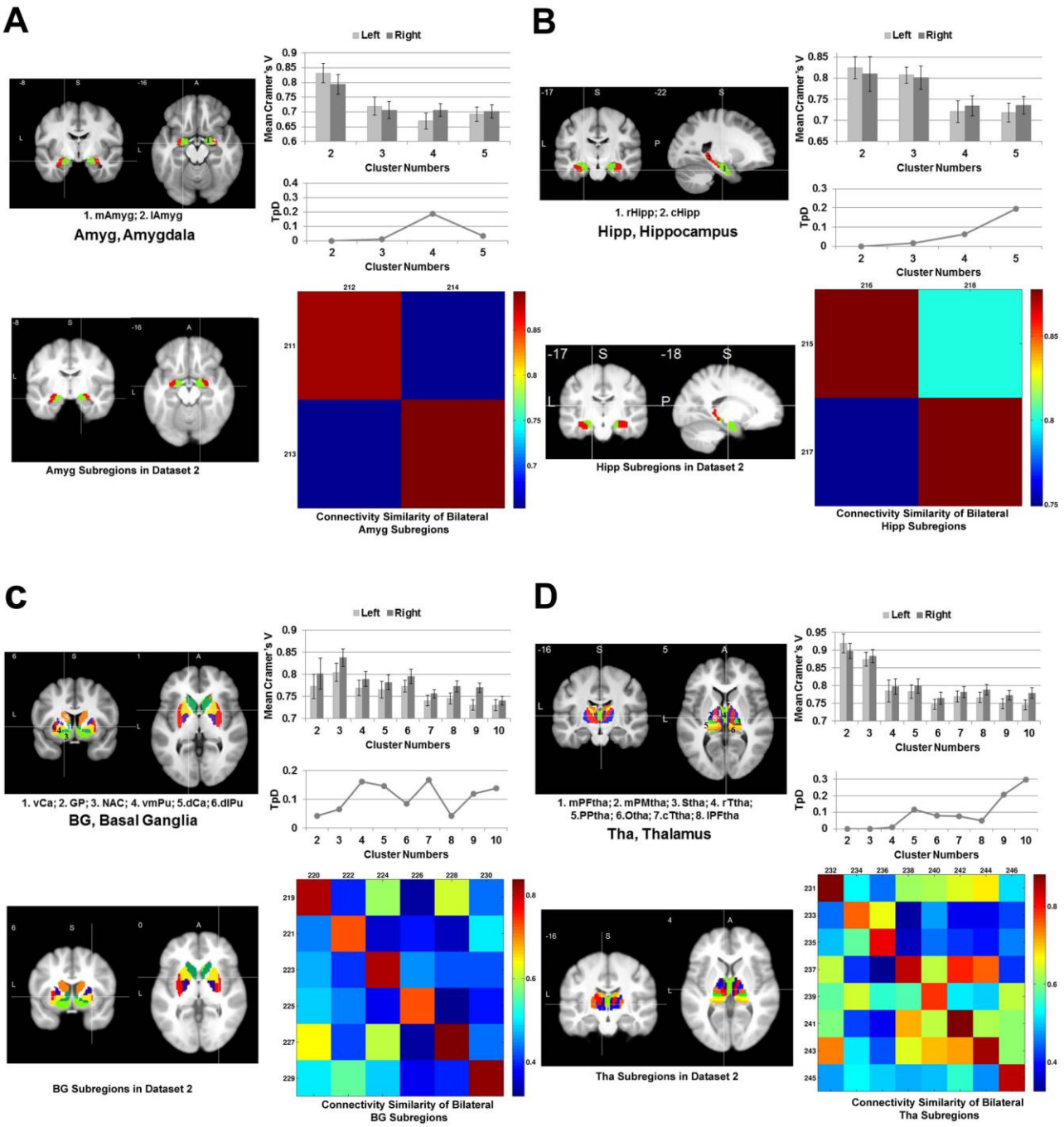

Figures S7. The Maximum Probability Maps of the Human Brainnetome Atlas Subregions in two Independent Datasets along with the Cramer's V, the Topological Distance (TpD), and the Connectivity Similarity Matrix of Bilateral Subregions: A. Amyg, Amygdala; B. Hipp, Hippocampus; C. BG, Basal Ganglia; D. Tha, Thalamus.